

Supplemental Informations:

1 Experimental section

1.1 Synthesis of BiVO₄ films

The BiVO₄ films were synthesized by a simple reaction method, which were divided into two steps. The first step was to configure a precursor solution containing Bi(NO₃)₃·5H₂O (5 mmol) and NH₄VO₃ (5 mmol), and the solvent was a mixed solution of deionized water and nitric acid (the volume ratio was 9: 1). Then, immerse the treated FTO (ultrasonically wash with acetone, isopropyl alcohol and ethanol for 30 minutes, respectively) into the solution obliquely with the conductive surface facing up, leaving a third of the blank. Next, it was heat-treated in a drying furnace with a constant temperature of 50 °C for 1 hour. The last step was to take out the yellow films and let it stand for a while, then wash it gently with absolute ethanol and deionized water several times and dry it for 20 minutes. After that, it was annealed at 450 °C for 2 h at a rate of 2 °C/min.

1.2 Synthesis of BiVO₄/CoNiO₂ films

The synthesis process was based on previous reports[S1]. First, a mixed aqueous solution (100 mL) of 0.6 g Ni(NO₃)₂·6H₂O, 0.6 g Co(NO₃)₂·6H₂O and 1.06 g urea was prepared and transferred to a Teflon-lined stainless-steel autoclave with BiVO₄ films. These autoclaves were then subjected to a 120 °C hydrothermal treatment for 3 h. After the reaction was completed and naturally cooled to room temperature, the products were taken out and washed with absolute ethanol and deionized water several times in turn, and then placed in a drying oven at 60 °C. Last, it was annealed at 300 °C for 2 h at a rate of 2 °C/min.

1.3 Characterization

Identification of the phase structures, constituent elements and valence states of all elements were performed by X-ray diffraction (XRD, Empyrem), X-ray photoelectron spectroscopy (XPS, Thermo ESCALAB 250XI, Al-K α) and energy dispersive X-ray spectrometer (EDS, Hitachi S4800), respectively. The surface morphology and interface matching of all samples were determined by scanning electron microscope (SEM, S4800, 5 kV) and transmission electron microscopy (TEM, Tecnai G2 F20). The photogenerated charge separation and transfer properties were characterized by surface photovoltage (SPV), photoluminescence (PL, FLS980) and electrochemical impedance spectroscopy (EIS, 5 mV, 0.01 Hz to 100 kHz). The absorbance was performed by DU-8B UV-vis double-beam spectrophotometer. The amount of hydrogen and oxygen

evolution was measured by a combination of a closed external photoreactor, an electrochemical workstation and a gas chromatograph. All of photoelectrochemical performance were performed by three-electrode electrochemical workstation (500 W xenon lamps with a UV filter). The as-obtained samples, Pt sheet, Ag/AgCl electrode and 0.5 M Na₂SO₄ aqueous solution were used as working electrode, counter electrode, reference electrode and electrolyte, respectively. Last, the results were converted to the reversible hydrogen electrode (RHE) according to the formula[S2]:

$$E_{\text{RHE}} = E_{\text{Ag/AgCl}} + 0.0591\text{pH} + 0.1976 \quad (1)$$

The incident photon-to-current conversion efficiency (IPCE) was calculated according to the formula[S3]:

$$\text{IPCE} = 1240 \times J / (\lambda \times P) \times 100\% \quad (2)$$

where J is the photocurrent density, λ is the incident-light wavelength, P is the incident-light power density.

The bias photon-to-current efficiency (ABPE) was calculated according to the formula[S4]:

$$\text{ABPE} = J (1.23 - V_b) / P \times 100\% \quad (3)$$

where J is the photocurrent density, V_b is the measured potential corresponding to the photocurrent, P is the incident-light power density.

The band gap of both photoanodes was based on the formula[S5]:

$$\alpha h\nu = A (h\nu - E_g)^n \quad (4)$$

where α is the absorption coefficient, h is the Planck constant, ν is the incident light frequency, A is the absorbance, E_g is the band gap and the value of n is 2 or 1/2. For BiVO₄ as an n-type indirect band gap semiconductor, n is 1/2.

Lists of the Figures:

Fig.S1 XRD pattern of BiVO_4 and $\text{BiVO}_4/\text{CoNiO}_2$

Fig.S2 XPS spectra of BiVO_4 and $\text{BiVO}_4/\text{CoNiO}_2$ for (a) Bi 4f and (b) V 2p

Fig.S3 XPS spectra of $\text{BiVO}_4/\text{CoNiO}_2$ after the water splitting for (a) Co 2p, (b) Ni 2p and (c) O 1s

Fig.S4 The EDS spectrum and all the elemental mapping images of $\text{BiVO}_4/\text{CoNiO}_2$

Fig.S5 The images of $\text{BiVO}_4/\text{CoNiO}_2$ after the water splitting: (a) SEM and (b) TEM

Fig.S6 The equivalent circuit of EIS spectrum

Fig.S7 (a) UV-vis absorption spectra and (b) Tauc plots of both photoanodes

Fig.S8 (a) Hydrogen evolution and (b) oxygen evolution curve measured under AM 1.5G continuous illumination

Fig.S9 The schematic illustration of the $\text{BiVO}_4/\text{CoNiO}_2$ photoanode

Table S1 Performance comparison of related materials

Table S2 The equivalent circuit fitting parameters

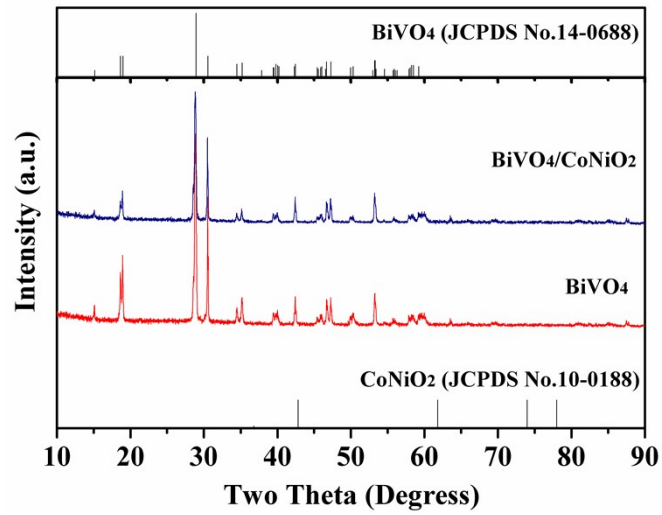


Fig.S1 XRD pattern of BiVO₄ and BiVO₄/CoNiO₂

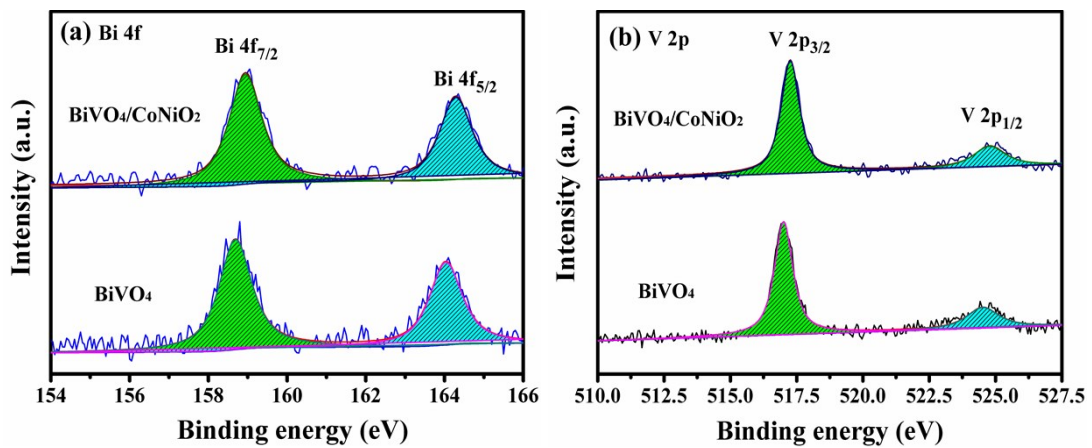


Fig.S2 XPS spectra of BiVO₄ and BiVO₄/CoNiO₂ for (a) Bi 4f and (b) V 2p

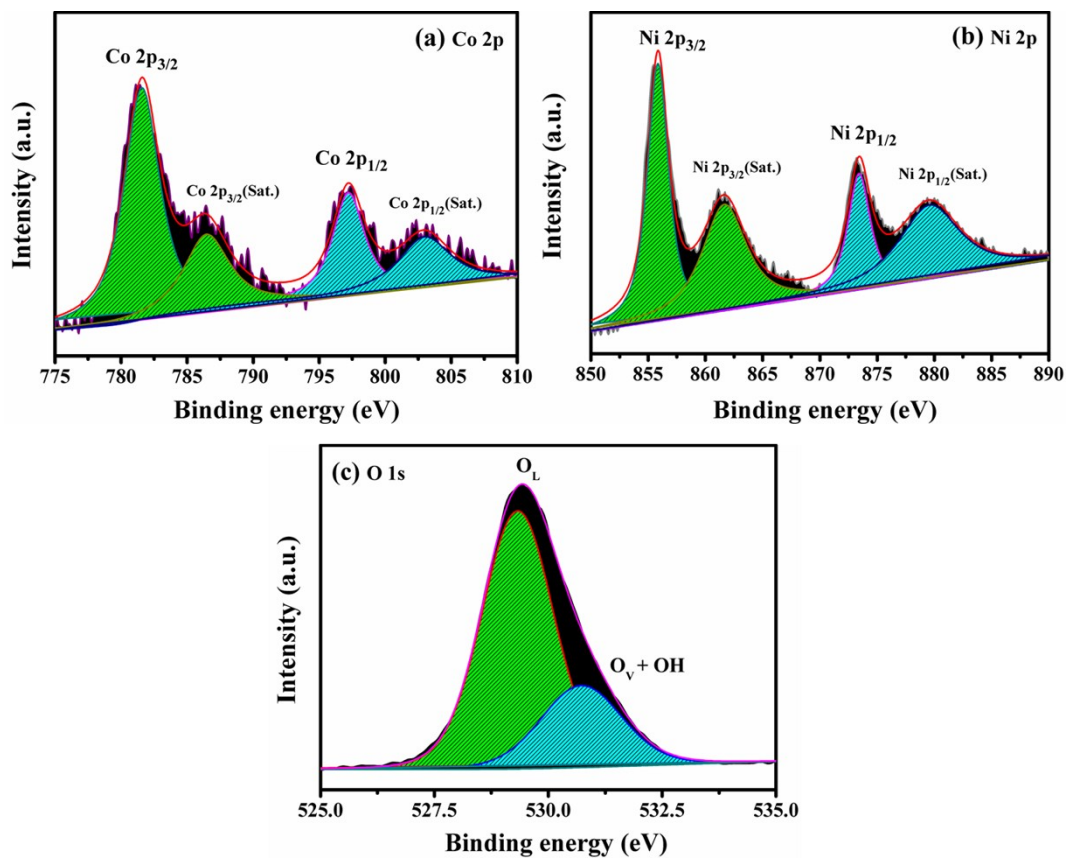


Fig.S3 XPS spectra of $\text{BiVO}_4/\text{CoNiO}_2$ after the water splitting for (a) Co 2p, (b) Ni 2p and (c) O 1s

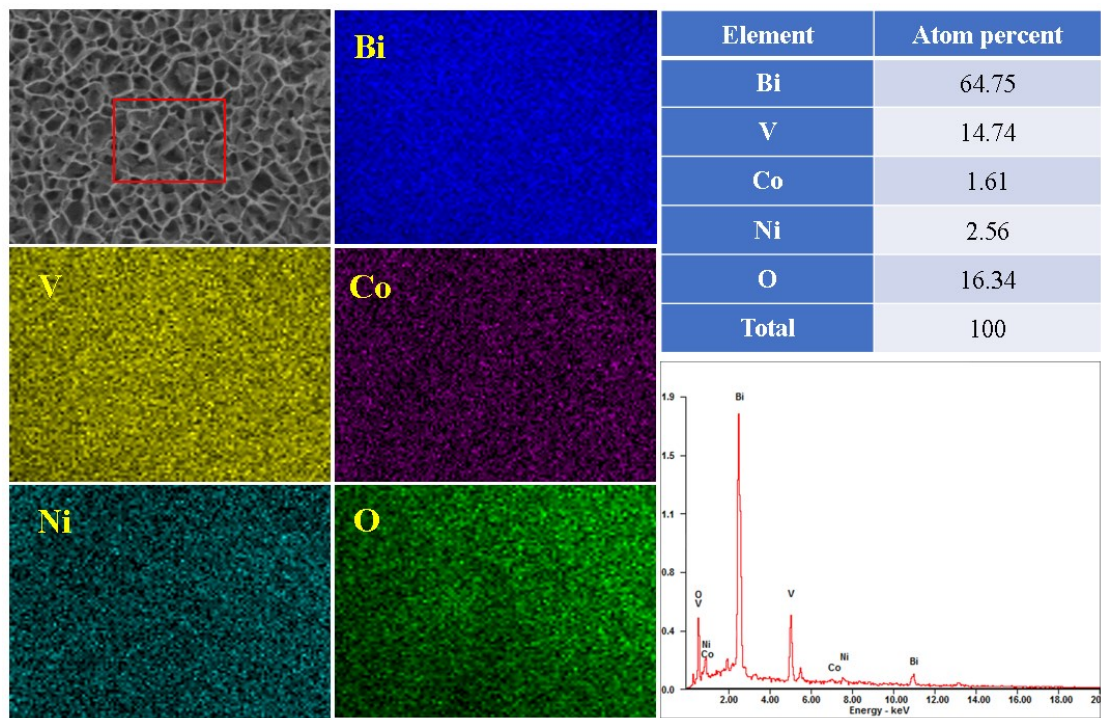


Fig.S4 The EDS spectrum and all the elemental mapping images of $\text{BiVO}_4/\text{CoNiO}_2$

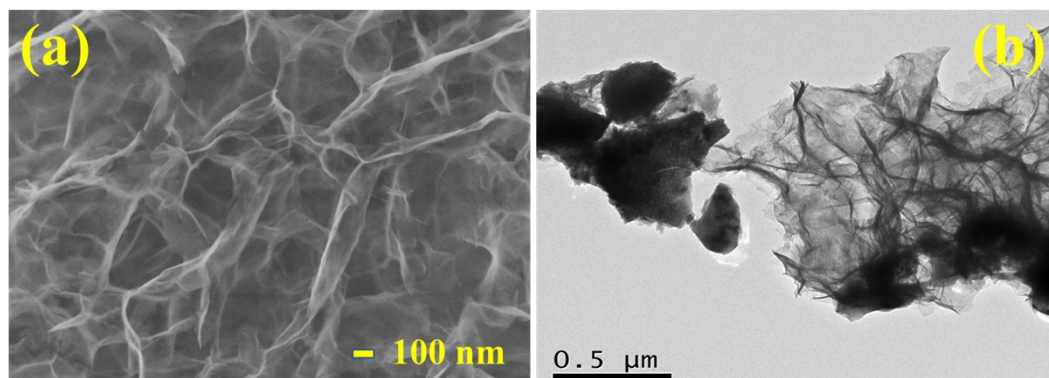


Fig.S5 The images of $\text{BiVO}_4/\text{CoNiO}_2$ after the water splitting: (a) SEM and (b) TEM

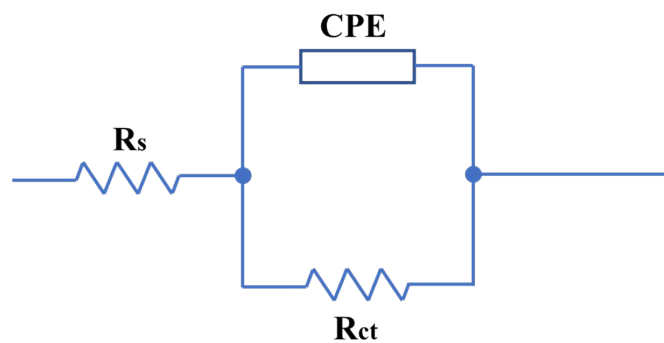


Fig.S6 The equivalent circuit of EIS spectrum

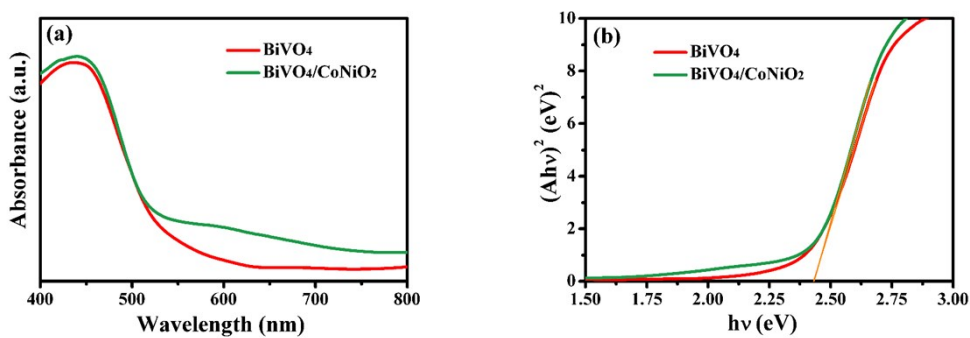


Fig.S7 (a) UV-vis absorption spectra and (b) Tauc plots of both photoanodes

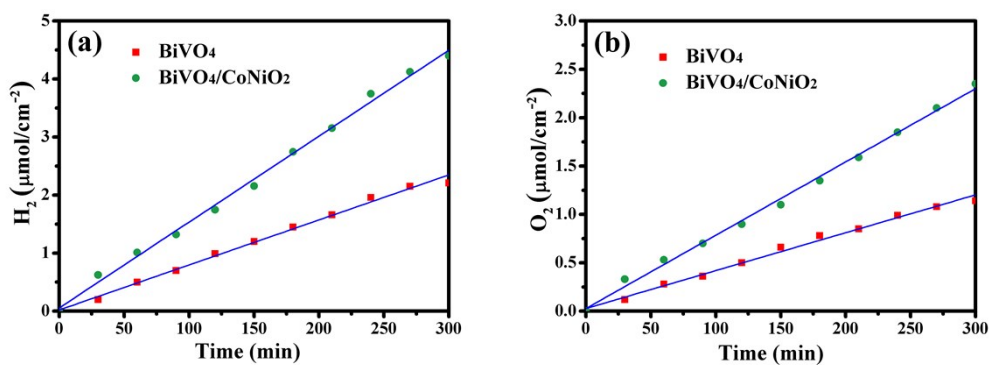


Fig.S8 (a) Hydrogen evolution and (b) oxygen evolution curve measured under AM 1.5G continuous illumination

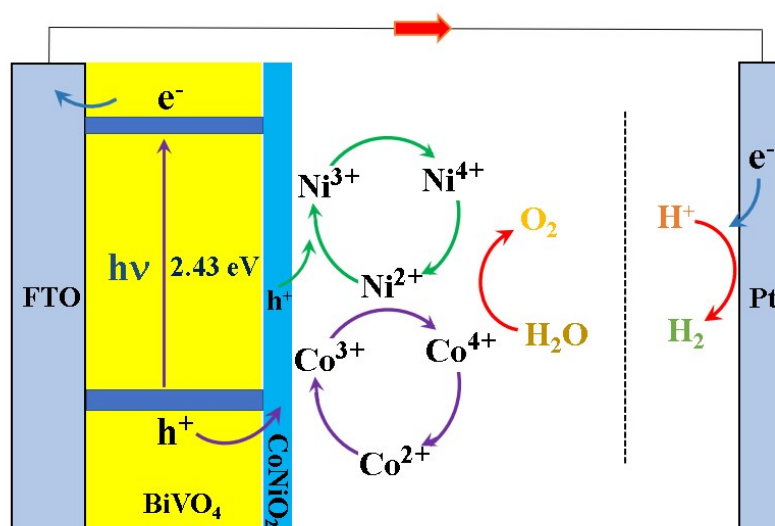


Fig.S9 The schematic illustration of the BiVO₄/CoNiO₂ photoanode

Table S1 Performance comparison of related materials

Photoanode	Fabrication method	Performance (electrolyte)
CoOOH/BiVO ₄ ^[S6]	Electrodeposition and hydrothermal method	4.0 mA/cm ² at 1.23 V vs. RHE (0.2 M potassium phosphate buffer solution containing 0.5 M Na ₂ SO ₄)
NiOOH/BiVO ₄ ^[S7]	Electrodeposition and impregnation	2.7 mA/cm ² at 1.23 V vs. RHE (1 M Na ₂ SO ₄ aqueous solution)
NiCo-LDH/BiVO ₄ ^[S8]	MOD and Electrodeposition	3.4 mA/cm ² at 1.23 V vs. RHE (0.5 M Na ₂ SO ₄ aqueous solution)
MFe ₂ O ₄ /BiVO ₄ ^[S9] (M = Ni, Co)	MOD and grinding calcinations method	0.65 mA/cm ² at 1.23 V vs. RHE (CoFe ₂ O ₄ /BiVO ₄) 0.35 mA/cm ² at 1.23 V vs. RHE (NiFe ₂ O ₄ /BiVO ₄) (0.5 M Na ₂ SO ₄ aqueous solution)
This work	Chemical solution deposition and hydrothermal method	1.16 mA/cm ² at 1.23 V vs. RHE (0.5 M Na ₂ SO ₄ aqueous solution)

Table S2 The equivalent circuit fitting parameters

Photoanode	R_s (Ω)	R_{ct} (Ω)	CPE (μF)
BiVO_4	225.2	7109	5.289
$\text{BiVO}_4/\text{CoNiO}_2$	126.9	3028	10.93

References:

- [S1] X.Q. Du, G.Y. Ma, X.S. Zhang. Dalton Transactions, 2019, 48: 10116-10121.
- [S2] M.R. Nellist, J.J. Qiu, F.A.L. Laskowski, F.M. Toma, S.W. Boettcher. Acs Energy Letters, 2018, 3: 2286-2291.
- [S3] Z.H. Zhang, M.F. Hossain, T. Takahashi. International Journal of Hydrogen Energy, 2010, 35: 8528-8535.
- [S4] D. Chen, Z.F. Liu. ChemSusChem, 2018, 11: 3438-3448.
- [S5] M.A. Butler. Journal of Applied Physics, 1977, 48: 1914-1920.
- [S6] F.M. Tang, W.R. Cheng, H. Su, X. Zhao, Q.H. Liu. Acs Applied Materials & Interfaces, 2018, 10: 6228-6234.
- [S7] H. Luo, C.H. Liu, Y. Xu, C. Zhang, W.C. Wang, Z.D. Chen. International Journal of Hydrogen Energy, 2019, 44: 30160-30170.
- [S8] H.D. She, P.F. Yue, X.Y. Ma, J.W. Huang, L. Wang, Q.Z. Wang. Applied Catalysis B-Environmental, 2020, 263: 118280.
- [S9] Q.Z. Wang, J.J. He, Y.B.A. Shi, S.L. Zhang, T.J. Niu, H.D. She, Y.P. Bi, Z.Q. Lei. Applied Catalysis B-Environmental, 2017, 214: 158-167.